J Mater Sci (2016) 51:8139–8147

ZrC formation and the phase relations in the Si–Zr–Mg–O–C system

W. Z. Sun[1,2,*], J. G. Cheng[1,*], Z. K. Huang[2], Y. Jiang[2], L. E. Wu[2], and L. M. Liu[2]

[1] School of Materials Science and Engineering, Hefei University of Technology, Hefei 230009, Anhui, People's Republic of China
[2] School of Materials Science and Engineering, Beifang University of Nationalities, Yinchuan 750021, Ningxia, People's Republic of China

Received: 30 March 2016
Accepted: 19 May 2016
Published online: 31 May 2016

ABSTRACT

When MgO+ZrO_2 were used as a sintering aid to SiC ceramics, it was found that ZrO_2 reacted with SiC and MgO to form ZrC and a magnesium silicate. This reaction may provide a new route to synthesize ZrC or prepare ZrC/SiC composites by reaction sintering using ZrO_2, SiC, and MgO as starting materials. In the present work, formation process of the ZrC phase in the SiC–MgO–ZrO_2 system was addressed. Subsolidus phase relations at 1550 °C of the SiC–MgO–ZrO_2 system and the related SiC–SiO_2–ZrC–ZrO_2–MgO (Si–Zr–Mg–O–C) system were investigated.

Introduction

ZrC-based ceramic as a member of the ultra-high temperature ceramic (UHTC) family [1, 2] has attracted increasing attention in recent years. A large number of documents are devoted to synthesis of UHTC powders and sintering of the UHTCs. For the synthesis of the UHTC powder, various techniques, such as carbon-thermal reduction [3], magnesium thermal reaction [4], self-propagation high-temperature synthesis [5], polymer-derived ceramics route [6–8], liquid precursor conversion method [9], to name a few, have been utilized to synthesize the ZrC powder. For the sintering of the UHTCs, due to high covalent bond of the ZrC compound, hot pressing and spark plasma sintering have to be applied to produce dense ZrC-based ceramics [10–16].

Combining both synthesis and sintering in one step via reaction sintering has long been thought as a good choice for producing dense UHTCs at a reasonably low cost [17]. Nachiappan et al. [18] exhibited synthesis and sintering zirconium carbide by reactive hot pressing, using C and the expensive metallic Zr powder as the raw materials. No other suitable reaction systems could be found in open literature.

In previous studies, we tried to use MgO+ZrO_2 as a sintering aid to the SiC ceramics in order to avoid the use of the costly rare-earth oxides (RE_2O_3) [19–21]. In the study, it was found that MgO and ZrO_2 reacted with SiC to form ZrC and a magnesium silicate by occasion. This reaction may provide a new reaction system for reaction sintering of the ZrC ceramics and/or ZrC/SiC composites [22–25]. It was obvious that developing such a reaction-sintering route requires details of the reactions and the phase

Address correspondence to E-mail: sun2422866@163.com; jgcheng63@sina.com

DOI 10.1007/s10853-016-0084-4

equilibria of the reaction system. Therefore, the phase relations of the SiC–MgO–ZrO_2 system and the related SiC–SiO_2–ZrC–ZrO_2–MgO (Si–Zr–Mg–O–C) system were investigated herein; the formation process of the ZrC phase in the system was also addressed. SiC usually is an inert substance and does not react with most of the oxides. However, reactions took place between SiC and ZrO_2 when MgO was present.

Experimental procedure

The starting powders were β-SiC (Grade UF-15-A, H. C. Starck, Germany. impurities contents: C ~ 29.0–30.0 %, O < 1.50 %, Al < 0.03 %, Ca < 0.01 %, Fe < 0.05 %; particle size $D_{50} = 0.55$ μm), SiO_2 (Aladdin Reagent Co., China. 99.9 % purity with average particle size ~5 μm), MgO (Aladdin Reagent Co., China. 99.9 % purity with average particle size ~3 μm), ZrC (Aladdin Reagent Co., China. 99.9 % purity with average particle size ~50 nm) and nano-ZrO_2 (Aladdin Reagent Co., China. 99.9 % purity with particle size ~100 nm). The oxide powders were calcined in air at 1100 °C for 1 h to remove hydrates before using. Powder mixtures in proper proportions were manually mixed with an agate pestle and mortar for 2 h in absolute alcohol as medium. After being dried, batches of the powder mixtures were dry-pressed at 70 MPa for 30 s in a mold with dimensions of 15 × 15 mm^2, followed by cold isostatic pressing at 250 MPa for 60 s to produce green samples with thickness ~5 mm. The samples were heated in a SiC/BN mixture powder bed in crucibles (either graphite or MgO crucibles) by a furnace (ZTY-50-23, Shanghai Rongcheng Electric Furnace Co. Ltd, China) with graphite heating elements. Heating of the ZrC-containing samples was carried out in 1 atm Ar at different temperatures for 3–5 h. The heating rate was 5–7 °C/min. After holding, the furnace was cooled at 7 °C/min to 1000 °C, followed by shut-down of the heating power for further cooling to room temperature. Heating conditions were adjusted according to the compositions of the samples to secure phase equilibrium. Phase equilibration at certain temperature was presumably reached when the phase compositions showed no more changes if the holding time was prolonged at that temperature.

About 1-mm material was ground off from a surface of the samples to eliminate possible contamination. The samples were sliced, ground, and polished to 1 μm finish. Phase compositions were analyzed by X-ray diffraction (XRD-6000, Shimadzu, Japan). Microstructures were observed by a scanning electron microscope (SEM, SHIMADZU, SSX-550) with energy dispersive X-ray spectroscopy (EDS). Thermodynamic calculation was done by using a software compact (HSC Chemistry 6.1, Outokumpu Research Oy, Pori, Finland).

Results and discussion

Phase relations in the SiC–ZrO_2–MgO ternary system and formation of the ZrC phase

The SiC–ZrO_2–MgO ternary system consisted of three binary subsystems, i.e., SiC–ZrO_2, SiC–MgO, and ZrO_2–MgO. The samples with a fixed composition of 1:1 mol ratio of the respective powders were solid-state reacted at 1600 °C to investigate the phase relations of the binary subsystems. XRD analyses showed no formation of any binary compounds in the SiC–ZrO_2 and SiC–MgO subsystems, demonstrating the inertness of SiC in the oxides. This observation on the binary phase formation in the ZrO_2–MgO subsystem was in consistency with the report in the literature [26].

Three compositions of SiC:MgO:ZrO_2 = 1:1:1, 1:2:1, 4:1:1 (noted as 1S1M1Z, 1S2M1Z, and 4S1M1Z, respectively) as shown in Table 1 were used to investigate the phase relations in the SiC–MgO–ZrO_2 ternary system. Samples were solid-state reacted at

Table 1 Phase compositions and weight loss of the ternary samples after solid-state reaction at 1600 °C in Ar

Materials	Compositions/mol ratios	Phase compositions by XRD	Weight loss (wt%)
1SC1M1Z	SiC:MgO:ZrO_2 = 1:1:1	ZrC, SiC(α), SiC(β), ZrO_2, Mg_2SiO_4	2.1
1SC1M1Z*	SiC:MgO:ZrO_2 = 1:1:1 (in MgO crucible)	ZrC, SiC(α), SiC(β), ZrO_2, Mg_2SiO_4	1.2
1SC2M1Z	SiC:MgO:ZrO_2 = 1:2:1	ZrC, Mg_2SiO_4	3.9
4SC1M1Z	SiC:MgO:ZrO_2 = 4:1:1	SiC(α), SiC(β), ZrC, ZrO_2, Mg_2SiO_4	4.7

The sample 1S1M1Z with symbol (*) was placed in a MgO crucible with lid. The sample 1S1M1Z without symbol (*) was placed in a graphite crucible

1600 °C in 1 atm Ar. XRD analysis results are listed in Table 1. The XRD pattern of the 1S2M1Z sample is shown in Fig. 1. In contrast to the binary subsystems, reactions occurred in all of the three ternary compositions to form new phases of ZrC and Mg_2SiO_4 (forsterite). The solid-reaction temperature was verified for the 1S1M1Z composition. The results demonstrated that the low temperature limit for the ZrC phase formation was at around 1250 °C.

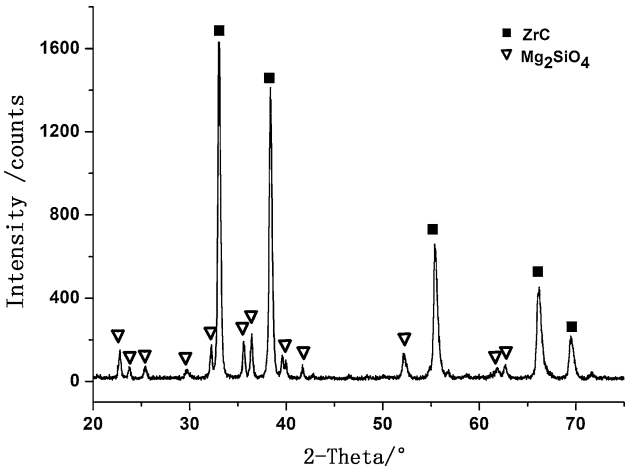

Figure 1 XRD pattern of the 1SC2M1Z (refer Table 1) composition after heated at 1600 °C.

Another note-worthy point in the XRD patterns was shifts of the peaks of the ZrC phase in all of the three samples relative to pure ZrC (PDF 658835). The chemical composition of the ZrC phase in the 1S2M1Z sample sintered at 1600 °C was analyzed by EDX in combination with SEM. The results are shown in Fig. 2. The SEM observations were in consistency with the XRD. Two phases having different image contrast and grain morphology were recognized on the micrographs. EDX analysis proved that the large dark grains were the Mg_2SiO_4 phase and the gray aggregates consisting of nano-sized grains were ZrC. The nano-ZrC grains were presumably resulted from nano-ZrO_2 as the raw material. A small amount of O and Si elements were detected in the ZrC areas, indicating dissolve of O and Si in the ZrC lattice to explain the XRD peak position shifts in Fig. 1.

Formation of the Mg_2SiO_4 phase could be attributed to reactions of MgO with the oxide impurity SiO_2 present on surfaces of the SiC particles by Reaction (1). Three possible routes to form the ZrC phase could be outlined. In the first route, SiC was

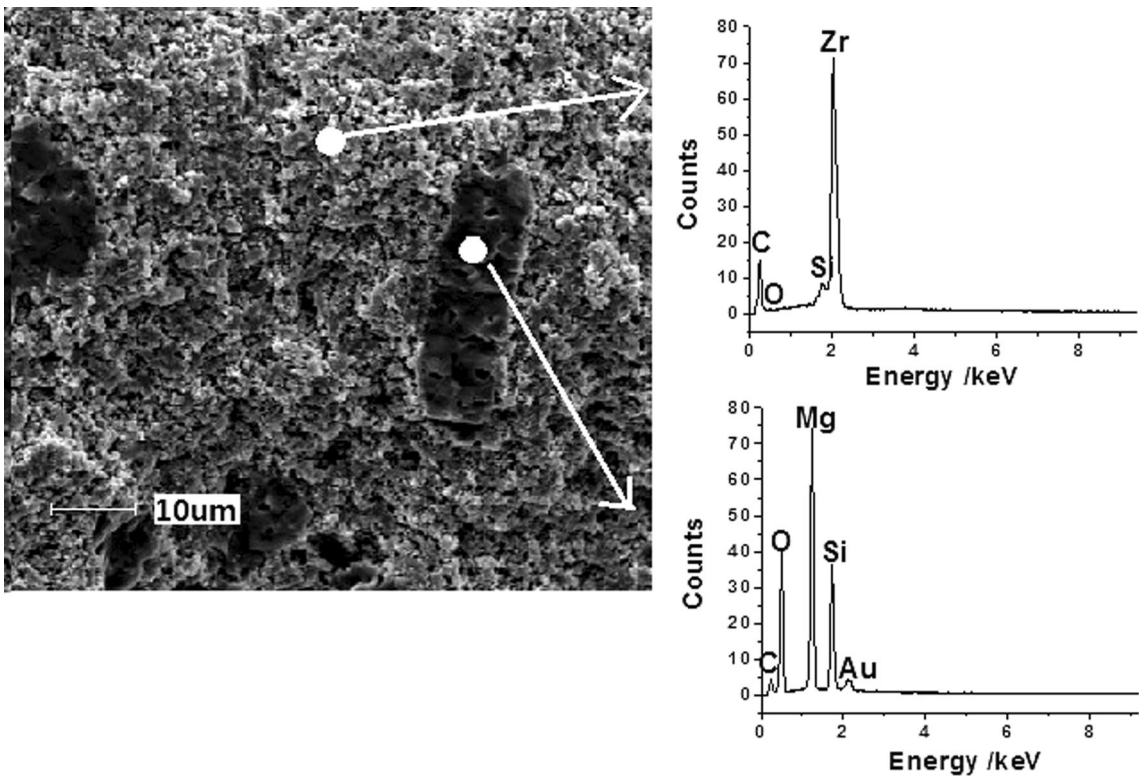

Figure 2 SEM micrograph and EDX spectrum of the 1SC1M1Z (refer Table 1) composition after heated at 1600 °C.

oxidized at high temperatures to generate CO by Reaction (2), and CO subsequently reacted with ZrO_2 to form ZrC by Reaction (3). In the second route, ZrO_2 reacted with carbon as Reaction (4) to form ZrC and CO. Carbon was abundant due to the graphite heating elements and the graphite crucibles in use. And in the third route, the members of the SiC–ZrO_2–MgO ternary system might undergo a direct solid-state reaction at high temperatures as Reaction (5).

$$SiO_2 + 2MgO \rightarrow Mg_2SiO_4, \quad (1)$$

$$SiC + 1.5O_2(g) \rightarrow SiO_2 + CO(g), \quad (2)$$

$$ZrO_2 + CO \rightarrow ZrC + 1.5O_2(g), \quad (3)$$

$$ZrO_2 + 3C \rightarrow ZrC + 2CO(g), \quad (4)$$

$$SiC + 2MgO + ZrO_2 \rightarrow ZrC + Mg_2SiO_4. \quad (5)$$

In order to insight into the formation process of the ZrC phase, the above Reactions (1–5) were examined by thermodynamic calculation from 200 to 2000 °C with a temperature interval of 200 °C. The results of the thermodynamic calculation are listed in Table 2. Reaction (2), i.e., the oxidation of SiC, had the lowest value of Gibbs free energy change ΔG [27] in the whole temperature range, suggesting that Reaction (2) could happen in the present experimental setup. The ΔG values for Reactions (3) were positive at all temperatures, while Reaction (4) was only favored at temperatures >1800 °C (Table 2). Reaction (5) had a small negative ΔG value in the temperature range and the ΔG value became more negative as the temperature increased, indicating Eq. (5) favorable.

Both the thermodynamic calculation and the experimental results confirmed the feasibility of Reaction (5) to form the ZrC and Mg_2SiO_4 phases. However, Reaction (5) could be derived by combining Reactions (1), (2), and (3). The standard free energy change ΔG for Reaction (5) at 1400 °C was −10.5 kJ/mol, the same value as the summary of Reactions (1), (2), and (3). On other hand, a reaction route of $SiC + ZrO_2 \rightarrow ZrC + SiO_2$ was formulated by combining Reactions (2) and (3), with a ΔG value as $-815.525 + 865.291 = +50$ kJ/mol, which means that this reaction was unable to be conducted. Since Reaction (5) consisted of Reactions (1), (2), and (3), Reaction (5) was the only one new route to produce ZrC and Mg_2SiO_4.

ΔG was the driving force for Reaction (5). According to the relations between the driving force and the kinetics of a reaction, the small negative ΔG for Reaction (5) would result in slow reaction rates, especially at low temperatures such as at 1250 °C. However, Reaction (5) may be favorably explained by the acid–base reaction theory because MgO is strongly basic, while SiC is acid and ZrO_2 is either weakly acid (e.g., in case of $CaZrO_3$) or weakly basic (e.g., in $ZrSiO_4$) depending on the coexistent substances. In fact, Reaction (5) consisted of two reactions as $SiC + ZrO_2 \rightarrow ZrC + SiO_2$ and $SiO_2 + 2MgO \rightarrow Mg_2SiO_4$. In fact, the former is a "double displacement reaction" which would not occur if MgO did not participate, and the latter was a "single displacement reaction," i.e., a real acid–base reaction that has been verified to occur in the previous sections [see Reaction (1)]. Therefore, Reaction (5) is a typical acid–base reaction due to the occurrence of the reaction $SiO_2 + 2MgO \rightarrow Mg_2SiO_4$. The rapid formation kinetics for ZrC and Mg_2SiO_4 at the low temperature limit of 1250 °C was thus explained by reactions of basic MgO with acidic $SiC + ZrO_2$.

Table 2 Calculation of the Gibbs free energy changes of Reactions (1–7)

T (°C)	ΔG_m1 (kJ)	ΔG_m2 (kJ)	ΔG_m3 (kJ)	ΔG_m4 (kJ)	ΔG_m5 (kJ)	ΔG_m6 (kJ)	ΔG_m7 (kJ)
200	−62.751	−909.382	970.377	511.402	−1.756	24.629	−36.366
400	−62.651	−892.858	952.276	438.933	−3.233	22.049	−37.368
600	−62.363	−876.76	934.336	367.21	−4.787	19.305	−38.271
800	−61.885	−861.061	916.535	296.338	−6.411	16.352	−39.121
1000	−61.174	−845.809	898.877	226.29	−8.107	13.442	−39.626
1200	−60.615	−830.64	881.533	157.179	−9.721	10.617	−40.277
1400	−60.264	−815.525	865.291	89.735	−10.498	8.936	−40.83
1600	−60.16	−800.452	849.095	22.857	−11.518	6.434	−42.209
1800	−59.94	−785.805	832.919	−43.519	−12.825	−3.439	−50.553
2000	−62.605	−771.936	816.741	−109.444	−17.8	−13.64	−58.446

ΔG_m n (n = 1, 2, 3, 4, 5, 6, 7) in the first entry of the table refer to Reaction (n) in the text

In order to investigate possible effect of carbon C (from the graphite crucible and the furnace), such as Reaction (4) on the formation of the ZrC phase, one sample with the 1S1M1Z (Table 1) composition was placed in a MgO crucible with lid, and another sample in a graphite crucible to calcine at 1600 °C. In both cases, the ZrC and Mg_2SiO_4 phases were formed, regardless of the isolation of the sample from the graphite by using the MgO crucible. This result suggested that carbon-thermal reduction of ZrO_2 was an unnecessary condition, different from Kljajevic et al. [28] where $ZrSiO_4$ was transformed into ZrO_2, SiC, and ZrC by carbon-thermal reduction. Mass losses of the samples before and after solid-state reaction at 1600 °C were measured and the results are listed in Table 1. All samples showed mass losses no more than 5 wt% (Table 1. The 4S1M1Z composition had the highest mass loss of up to 4.7 wt%.) If the ZrC phase was formed by Reactions (3) and (4), i.e., involving CO and C, the mass losses would be much higher, according to theoretical calculations. For example, the mass loss for the 1SC1M1Z composition would reach 23.57 and 15.72 wt% by Reaction (3) and (4), respectively, in contrast to the recorded <2.1 wt% (see Table 1). This mass loss examination further illustrated that the ZrC phase was formed neither by the Reaction (3) nor by Reaction (4). However, in the following experiments, a powder mixture of SiC/BN was used as a powder bed to cover samples during solid-state reaction, in order to reduce mass losses of the samples, even small and insignificant, by solid-state Reaction (5).

There are two magnesium silicates, namely Mg_2SiO_4 and $MgSiO_3$, existing in the MgO–SiO_2 system. Reaction (5) produced the Mg_2SiO_4 phase with the absence of $MgSiO_3$. If the $MgSiO_3$ phase was presumably generated by the following Reaction (6), thermodynamic calculation showed that the ΔG value for Reaction (6) was negative only at temperatures >1800 °C, well beyond the melting point temperature of the $MgSiO_3$ phase. Therefore, the $MgSiO_3$ phase should not be present under our experiment conditions (≤1600 °C). Mg_2SiO_4 was the only feasible phase. This analysis explained the appearance of the Mg_2SiO_4 phase with the absence of $MgSiO_3$, suggesting easier formation of the Mg-rich silicate of Mg_2SiO_4 instead of $MgSiO_3$.

$$SiC + MgO + ZrO_2 \rightarrow ZrC + MgSiO_3. \quad (6)$$

The phase compositions of the samples seemed dependent on the SiC:MgO:ZrO_2 ratios. The 1SC2M1Z sample had a SiC:MgO:ZrO_2 ratio of 1:2:1 to match Reaction (5). Accordingly, Mg_2SiO_4 and ZrC were the only reaction products detected by XRD. In contrast, the 1SC1M1Z and 4SC1M1Z compositions had a SiC:MgO:ZrO_2 ratio of 1:1:1 and 4:1:1, respectively. Excess SiC and ZrO_2 were detected in the 1SC1M1Z and 4SC1M1Z materials (Table 1).

According to the above analysis, only Reaction (5) could be used to produce the UHTC of ZrC with some Mg_2SiO_4 as the secondary phase by a solid-state reaction route. In industry, ZrC was commonly synthesized by carbon-thermal reduction of ZrO_2. The carbon-thermal reduction reaction was referred to Reaction (4) which was thermodynamically favorable only at temperatures >1800 °C. However, the present experiment evidenced that ZrC could be formed at a much lowered temperature of 1250 °C by Reaction (5), to provide an economical route for synthesizing ZrC.

The solid-state Reaction (5) as a new route to direct synthesis of ZrC had obvious advantages of fourfolds. The first was the avoidance of using ZrC powder as the starting material to fabricate the ZrC ceramics. The second was the introducing of some liquid into the sintering system by reaction of MgO and SiO_2, which would obviously favor densification of the ZrC-based materials. The third advantage was the Mg_2SiO_4 compound. It has a melting temperature of up to 1900 °C. Therefore, the presence of Mg_2SiO_4 as a secondary phase in the ZrC composites may benefit high-temperature oxidation resistance of the ZrC-based ceramics. And the forth, the solid-state Reaction (5) could produce ZrC at a temperature as low as 1250 °C, thus avoiding volatilization of the MgO substance at high temperatures [29, 30].

However, it should be pointed out that the ZrC yield as a product of Reaction (5) was only 42 wt% (i.e., ZrC:Mg_2SiO_4 = 1:1 in molar ratio), too small to form ZrC-based UHTC composites. Fortunately, addition of more SiC and ZrO_2 along with suitable amounts of MgO/Mg would increase the ZrC content, as shown by the following Reactions (7) and (8) for example. The thermodynamic calculations for Reaction (7) are listed in Table 3. It was evidenced that Reactions (7) and (8) are favorable at temperatures >1400 °C to produce ~60 wt% ZrC and at temperatures >1500 °C to produce ~70 wt% ZrC, respectively. Hot pressing (HP) or sintering in sealed containers could help alleviate mass loss of the MgO/Mg substances at high temperatures.

Table 3 Phase compositions of the quaternary samples after solid-state reaction at 1600 °C in Ar

Materials	Compositions/mol ratios	Phase compositions by XRD
1S5S'2M2Z	$SiC:SiO_2:MgO:ZrO_2 = 1:5:2:2$	SiC, SiO_2, $MgSiO_3$, $ZrSiO_4$
1S2S'1M1Z	$SiC:SiO_2:MgO:ZrO_2 = 1:2:1:1$	SiC, $MgSiO_3$, $ZrSiO_4$
2S3S'5M1Z	$SiC:SiO_2:MgO:ZrO_2 = 2:3:5:1$	SiC, Mg_2SiO_4, $ZrSiO_4$, ZrO_2
1S2S'2M1Z	$SiC:SiO_2:MgO:ZrO_2 = 1:2:2:1$	SiC, $ZrSiO_4$, Mg_2SiO_4
2S1S'5M1Z	$SiC:SiO_2:MgO:ZrO_2 = 2:1:5:1$	SiC, Mg_2SiO_4, ZrC, MgO

$$2SiC + 2ZrO_2 + MgO + Mg = 2ZrC + Mg_2SiO_4 + SiO(g), \quad (7)$$

$$3SiC + 3ZrO_2 + 2Mg = 3ZrC + Mg_2SiO_4 + 2SiO(g). \quad (8)$$

In addition to MgO, we found other alkaline oxides, i.e., CaO, SrO, BaO, as well as some light rare-earth oxides, also could be effective in producing UHT carbides MC where M referred to the IV group elements of Ti, Zr, Hf, as well as WC. These reactions will be studied in future works.

Phase relations in the $SiC–SiO_2–ZrC–ZrO_2–MgO$ (Si–Zr–Mg–O–C) quinary system

As have been discussed in the previous sections, Reaction (5) in the $SiC–MgO–ZrO_2$ ternary system could produce ZrC and Mg_2SiO_4, the latter having a high melting point temperature reaching 1900 °C. However, these two reaction products were not included in the phase diagrams of the ternary system. In addition, a well-known SiO_2 is a factor that cannot be ignored during sintering of both SiC ceramics and ZrC/SiC composites [31], because SiO_2 causes formation of silicates and changes the phase relations in the respective systems. Accordingly, phase relations in the $SiC–SiO_2–ZrC–ZrO_2–2MgO$ (Si–Zr–Mg–O–C) quinary system were investigated in order to understand the phase relations of ZrC with the neighboring phases in the system for compositional design of the ZrC-based composites.

The $SiC–MgO–ZrO_2–SiO_2$ subsystem

The $SiC–MgO–ZrO_2$ triangle separates the quinary system into two parts: $SiC–MgO–ZrO_2–SiO_2$ and $SiC–MgO–ZrO_2–ZrC$. The former $SiC–MgO–ZrO_2–SiO_2$ quaternary system contains four ternary systems, i.e., $SiC–MgO–ZrO_2$, $SiC–MgO–SiO_2$, $SiC–ZrO_2–SiO_2$, and $ZrO_2–MgO–SiO_2$. As the $SiC–MgO–ZrO_2$ system had been described in the above sections, the other two SiC-containing systems were detailed hereafter.

In the $SiC–ZrO_2–SiO_2$ and $ZrO_2–MgO–SiO_2$ systems, it was determined that no reaction took place between SiC and the oxides [32], introducing the $SiC–MgSiO_3$ and $SiC–Mg_2SiO_4$ tie-lines in the $SiC–MgO–SiO_2$ system and the $SiC–ZrSiO_4$ tie-line in the $SiC–ZrO_2–SiO_2$ system. The phase diagrams of these subsystems were established in our previous works [32]. And the phase diagram of the $ZrO_2–MgO–SiO_2$ system is shown in Fig. 3 [33]. Only three binary compounds, i.e., Mg_2SiO_4 (forsterite), $MgSiO_3$ (protoenstatite), and $ZrSiO_4$ (zirconite), were detected. Their coexistent relations constituted three tie-lines of $MgSiO_3–ZrSiO_4$, $ZrSiO_4–Mg_2SiO_4$, and $Mg_2SiO_4–ZrO_2$. These tie-lines separated the $ZrO_2–MgO–SiO_2$ system into four triangles. According to the above experimental results, five samples with different compositions (Table 3) in the $SiC–MgO–ZrO_2–SiO_2$ quaternary system were prepared at 1550 °C. Their XRD analysis results are listed in Table 3. All the oxide phases in the $ZrO_2–MgO–SiO_2$ ternary system were in equilibrium with SiC, forming four four-phase coexistent regions in the quaternary system, i.e.,

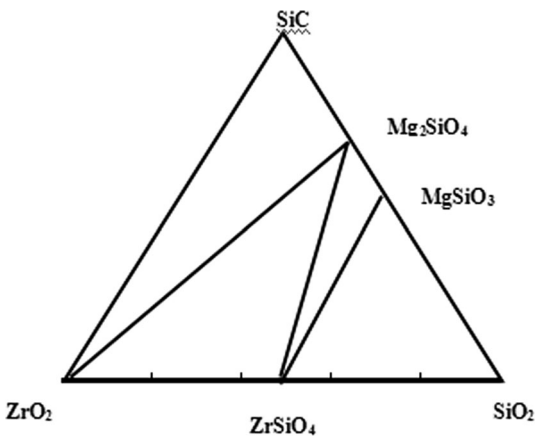

Figure 3 Subsolidus phase diagram of the $SiO_2–MgO–ZrO_2$ ternary system at 1450 °C [33].

$$\begin{aligned} &SiC - MgSiO_3 - ZrSiO_4 - SiO_2;\\ &SiC - MgSiO_3 - ZrSiO_4 - Mg_2SiO_4;\\ &SiC - Mg_2SiO_4 - ZrSiO_4 - ZrO_2;\\ &SiC - Mg_2SiO_4 - ZrO_2 - 2MgO. \end{aligned}$$

XRD patterns of the 1S5S′2M2Z and the 2S1S′5M1Z samples (Table 3) demonstrated four-phase coexistence regions as shown in Fig. 4. The results shown in

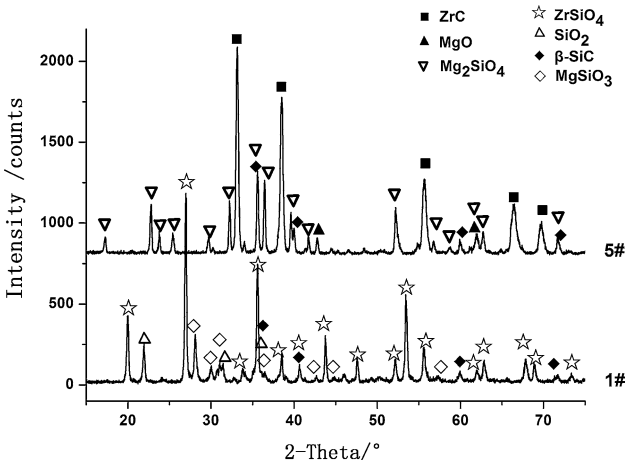

Figure 4 XRD pattern of the 1S5S′2M2Z and 2S1S′5M1Z (refer Table 3) compositions after heated at 1500 °C.

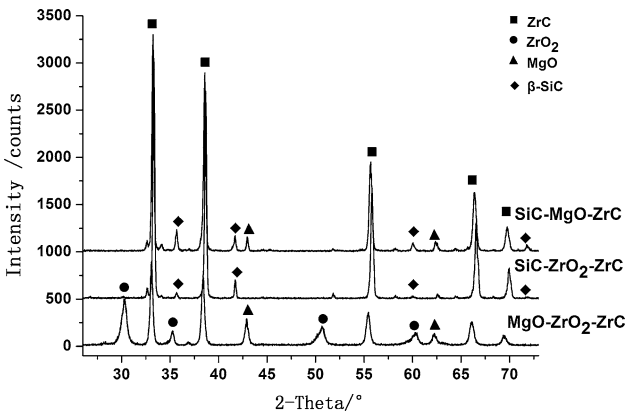

Figure 5 XRD patterns of the samples in the MgO–ZrO_2–ZrC, SiC–ZrO_2–ZrC, and SiC–MgO–ZrC ternary systems.

Table 3 indicated that the samples with lower MgO contents (for example, in the 1S5S′2M2Z and 1S2S′1M1Z compositions, Table 3) were easy to form $MgSiO_3$ and $ZrSiO_4$ by Reaction (9); however, the MgO-richer 2S3S′5M1Z, 1S2S′2M1Z, and 2S1S′5M1Z samples favored the formation of the Mg_2SiO_4 and ZrC phase along with $ZrSiO_4$. This observation implied that MgO reacted with SiO_2 to form $MgSiO_3$ in the first stage, and then excess MgO participated in Reaction (5) to promote the ZrC formation and further to form Mg_2SiO_4.

$$MgO + SiO_2 \rightarrow MgSiO_3. \quad (9)$$

The thermodynamic calculation results (Table 2) showed that only Reactions (1), (5), and (9) had negative ΔG values from 200 to 2000 °C, where the ΔG values of Reaction (5) was higher than those of Reactions (1) and (9), indicating reactions to be more favorable by Reactions (1) and (9) than by Reaction (5). This analysis demonstrated that reactions of SiO_2 impurity to form the magnesium silicates preceded the formation of the ZrC phase and Mg_2SiO_4 by Reaction (5).

The SiC–MgO–ZrO_2–ZrC subsystem

The SiC–MgO–ZrO_2–ZrC quaternary system consisted of four ternary subsystems: MgO–ZrO_2–ZrC, SiC–ZrO_2–ZrC, SiC–MgO–ZrC, and SiC–MgO–ZrO_2 (The SiC–MgO–ZrO_2 system had been described in the previous sections.) Three compositions with a 1:1:1 mol ratio (the compositions were laid in the respective ternary systems) were sintered at 1550 °C. The XRD patterns of the samples are shown in Fig. 5. It was shown that no binary reaction happened between the end members in the three systems. Nevertheless, in the XRD pattern of the sample which was representative for the SiC–ZrO_2–ZrC system, the XRD peaks of the ZrC phase showed a significant position shift (Table 4). According to the EDX results, O and Si elements were revealed in the ZrC lattice to explain this XRD peak position shift.

Table 4 Selected 2θ values of the XRD peaks of the ZrC phase in 2S1S′5M1Z sample and of the pure ZrC (picked up from PDF 35-0784)

2θ (degrees)	(111)	(200)	(220)	(311)	(222)
Of the pure ZrC	33.040	38.337	55.323	65.967	69.304
Of the 2S1S′5M1Z sample	33.321	38.661	55.820	66.599	69.979
$\Delta 2\theta$	0.281	0.324	0.497	0.632	0.675

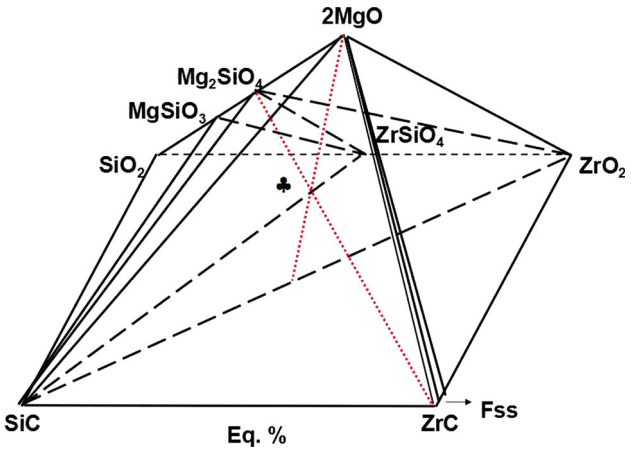

Figure 6 Subsolidus phase diagram of the SiC–SiO_2–MgO–ZrO_2–ZrC system at 1550 °C. ♣ is the barycentre of the SiC–ZrO_2–2MgO triangle.

The SiC–SiO_2–ZrC–ZrO_2–2MgO quinary system

Summarizing the results described in the above sections, the phase diagram of the SiC–SiO_2–ZrC–ZrO_2–2MgO quinary system at 1550 °C could be constructed, as presented in Fig. 6. SiC was in equilibrium with each of the three oxides of SiO_2, ZrO_2, and MgO and their silicates, as well as ZrC, forming five four-phase coexistent regions in system, i.e.,

$$\begin{aligned} &SiC - MgSiO_3 - ZrSiO_4 - SiO_2;\\ &SiC - MgSiO_3 - ZrSiO_4 - Mg_2SiO_4;\\ &SiC - Mg_2SiO_4 - ZrSiO_4 - ZrO_2;.\\ &ZrC - Mg_2SiO_4 - SiC - 2MgO;\\ &ZrC - Mg_2SiO_4 - ZrO_2 - 2MgO. \end{aligned}$$

Within the SiC–2MgO–ZrO_2 system, the gravity point of the ternary system had a composition of 1:2:1 in mole ratio. The ZrC–Mg_2SiO_4 tie-line crossed the gravity point of the SiC–2MgO–ZrO_2 triangle. In addition, according to references [34] oxygen ions could exist in the ZrC lattice to form a solid solution of ZrC_xO_y. So the solid solution of ZrC_xO_y was also marked in the phase diagram (Fig. 6). The established phase relations of this quinary system may contribute to compositional design for manufacture of the ZrC-based ceramics or the ZrC/SiC composites by solid-state reaction. The three triangles ZrC–SiC–Mg_2SiO_4, ZrC–SiC–MgO, and ZrC–SiC–ZrO_2 as well as the quaternary systems in this quinary system will be of specific importance.

Conclusions

The solid-state reaction of SiC + 2MgO + ZrO_2 → ZrC + Mg_2SiO_4 was analyzed in detail. ZrC could be formed at a much lowered temperature of 1250 °C relative to synthesizing of ZrC powder by carbonthermal reduction. The solid-state reaction mechanism was investigated by means of thermodynamic calculation, chemical kinetics, and experimental verification.

The phase relations of the SiC–SiO_2–ZrC–ZrO_2–2MgO (Si–Mg–Zr–O–C) quinary system were determined to confirm that SiC was in equilibrium with the three oxide members and their silicates, as well as ZrC, to form five four-phase coexistent regions in the system.

The phase diagram of the SiC–SiO_2–ZrC–ZrO_2–2MgO quinary system at 1550 °C was presented. We hope it will contribute to compositional design for the manufacture of the ZrC-based ceramics or the ZrC/SiC composites by solid-state reaction.

Acknowledgements

Y. Jiang and L. M. Liu acknowledge the financial support by the National Natural Science Foundation of China under Grant Nos. NSFC51362001 and NSFC5127205, respectively.

References

[1] Ma BX, Han WB, Guo EJ (2014) Oxidation behavior of ZrC-based composites in static laboratory air up to 1300°C. Int J Refract Met Hard Mater 46:159–167

[2] Wang XF, Liu JC, Hou F, Hu JD, Sun X, Zhou YC (2015) Synthesis of ZrC–SiC powders from hybrid liquid precursors with improved oxidation resistance. J Am Ceram Soc 98(1):197–204

[3] Li F, Huang X, Zhang GJ (2015) Scalable foaming assisted synthesis of ZrC nanopowder by carbothermal reduction. Ceram Int 41:3335–3338

[4] Davoodi D, Hassanzadeh-Tabrizi SA, Emami AH, Salahshour S (2015) A low temperature mechanochemical synthesis of nanostructured ZrC powder by a magnesiothermic reaction. Ceram Int 41:8397–8401

[5] Hajalilou A, Hashim M, Kamari HM, Javadi K, Kanagesaan S, Parastegari M (2014) Synthesis of ZrC nanoparticles in the ZrO-Mg-C-Fe system through mechanically activated

self-propagating high temperature synthesis. Acta Metall 27(6):1144–1151

[6] Liu CQ, Li KZ, Li HJ, Zhang SY, Zhang YL, Hou XG (2015) Synthesis, characterization, and ceramization of a SiC-ZrC-C preceramic polymer precursor. J Membr Sci 50(7):2824–2831

[7] Pizon D, Lucas R, Foucaud S, Maitre A (2011) ZrC-SiC materials from the polymer-derived ceramics route. J Am Ceram Soc 12(7):599–603

[8] Cai T, Qiu WF, Liu D, Han WJ, Ye L, Zhao AJ, Zhao T (2013) Synthesis of ZrC-SiC powders by a preceramic solution route. J Am Ceram Soc 96(10):3023–3026

[9] Liu D, Qiu WF, Cai T, Sun YN, Zhao AJ, Zhao T (2014) Synthesis, characterization, and microstructure of ZrC/SiC composite ceramics via liquid precursor conversion method. J Am Ceram Soc 97(4):1242–1247

[10] Nunez-Gonzalez B, Ortiz AL, Guiberteau F, Nygren M (2012) Improvement of the spark-plasma-sintering kinetics of ZrC by high-energy ball-milling. J Membr Sci 95(2):453–456

[11] Acicbe RB, Goller G (2013) Densification behavior and mechanical properties of spark plasma-sintered ZrC-TiC and ZrC-TiC-CNT composites. J Membr Sci 48(6):2388–2393

[12] Licheri R, Orrù R, Musa C, Cao G (2008) Combination of SHS and SPS techniques for fabrication of fully dense ZrB_2-ZrC-SiC composites. Mater Lett 62:432–435

[13] Li ZQ, Li HJ, Zhang SY, Li KZ (2012) Microstructure and ablation behaviors of integer felt reinforced C/C–SiC–ZrC composites prepared by a two-step method. Ceram Int 38:3419–3425

[14] Wu WW, Zhang GJ, Kan YM, Wang PL, Vanmeensel K, Vleugels J, Biest Omer VD (2007) Synthesis and microstructural features of ZrB_2-SiC-based composites by reactive spark plasma sintering and reactive hot pressing. Scr Mater 57:317–320

[15] Zhang Y, Gao D, Xu CL, Song Y, Shi XB (2014) Oxidation behavior of hot pressed ZrB_2-ZrC-SiC ceramic composites. Int J Appl Ceram Technol 11(1):178–185

[16] Kirilenko EV, Derii AI, Petrovskii VYa (2009) Dependence of the resistivity of hot-pressed Si_3N_4-ZrC composites on their composition. Powder Metall Met Ceram 48(9-10):560–568

[17] Tamoghna C et al (2014) Effect of zirconium on the densification of reactively hot-pressed zirconium carbide. J Am Ceram Soc 97(10):3092–3102

[18] Nachiappan C, Rangaraj L, Divakar C, Jayaram V (2010) Synthesis and densification of monolithic zirconium carbide by reactive hot pressing. J Am Ceram Soc 93(5):1341–1346

[19] Liang HQ, Yao XM, Zhang JX, Liu XJ, Huang ZG (2014) The effect of rare earth oxides on the pressureless liquid phase sintering of α-SiC. J Eur Ceram Soc 34:2865–2874

[20] Rodríguez-Rojas F, Ortiz AL, Borrero-López OB, Guiberteau F (2012) Effect of the sintering additive content on the protective passive oxidation behaviour of pressureless liquid-phase-sintered SiC. J Eur Ceram Soc 32:3531–3536

[21] Neher R, Herrmann M, Brandt K, Jaenicke-Roessler K, Pan Z, Fabrichnaya O, Seifer HJ (2011) Liquid phase formation in the system SiC, Al_2O_3, Y_2O_3. J Eur Ceram Soc 31:175–181

[22] Jiang JM, Wang S, Li W, Chen ZH, Zhu YL (2014) Preparation of 3D C_f/ZrC–SiC composites by joint processes of PIP and RMI. Mater Sci Eng A 607:334–340

[23] Zhao LY, Jia DC, Duan XM, Yang ZH, Zhou Y (2012) Oxidation of ZrC–30 vol% SiC composite in air from low to ultrahigh temperature. J Eur Ceram Soc 32:947–954

[24] Song CB, Lin TS, He P, Yang WQ, Jia DC, Feng JC (2014) Microstructure evolution and its effect on the mechanical properties of the ZrC–SiC composite joint diffusion bonded with pure Ni foil. Ceram Int 40:17–23

[25] El-Sheikh SM, Zaki ZI, Ahmed YMZ (2014) In situ synthesis of ZrC/SiC nanocomposite via carbothermic reduction of binary xerogel. J Alloys Compd 613:379–386

[26] Du Y, Jin ZP (1991) Optimization and calculation of the ZrO2-MgO system CALPHAD. Comput Coupling Phase Diagr Thermochem 15(1):59–68

[27] Negita K (1986) Effective sintering aids for silicon carbide ceramics: reactivities of silicon carbide with various additives. J Am Ceram Soc 69(12):C308–C310

[28] Lj Kljajevic B, Matovic A Rsdosavljevic-Mihajlovic, Rosic M, Boskovic S, Devecerski A (2011) Preparation of ZrO_2 and ZrO_2/SiC powders by carbothermal reduction of $ZrSiO_4$. J Alloys Compd 509:2203–2215

[29] Tatli Z, Thompson DP (2007) The use of MgO-coated SiC powders as low temperature densification materials. J Eur Ceram Soc 27:1313–1317

[30] Foster D, Thompson DP (1999) The Use of MgO as a Densification Aid for α-SiC. J Eur Ceram Soc 19:2823–2831

[31] Li D, Yao XM, Chen J, Jiang F, Yang Y, Huang ZG, Liu XJ (2013) Microstructure and reaction mechanism of SiC ceramic with mullite-zircon as a new liquid-phases sintering additives system. Mater Sci Eng A 559:510–514

[32] WZ Sun, LE Wu, Y Jiang, ZK Huang, JG Cheng Phase relations in the SiC-SiO_2-M_xO_y (M_xO_y: MgO,Al_2O_3,ZrO_2) systems (submitted)

[33] Foster WR (1951) Contribution to the interpretation of phase diagrams by ceramists. J Am Ceram Soc 34(5):151–160

[34] Gozzi D, Montozzi M, Cignini PL (1999) Apparent oxygen solubility in refractory carbides. Solid State Ionics 123:1–10